AIP | Journal of Applied Physics

A study of the phase diagram of (K,Na,Li)NbO3 determined by dielectric and piezoelectric measurements, and Raman spectroscopy

Naama Klein, Evelyn Hollenstein, Dragan Damjanovic, H. J. Trodahl, Nava Setter et al.

Citation: J. Appl. Phys. **102**, 014112 (2007); doi: 10.1063/1.2752799
View online: http://dx.doi.org/10.1063/1.2752799
View Table of Contents: http://jap.aip.org/resource/1/JAPIAU/v102/i1
Published by the AIP Publishing LLC.

A study of the phase diagram of $(K,Na,Li)NbO_3$ determined by dielectric and piezoelectric measurements, and Raman spectroscopy

Naama Klein,[a] Evelyn Hollenstein, Dragan Damjanovic, H. J. Trodahl,[b] and Nava Setter
Ceramics Laboratory, Swiss Federal Institute of Technology—EPFL, Lausanne 1015, Switzerland

Martin Kuball
Applied Spectroscopy Group, H.H. Wills Physics Laboratory, University of Bristol, Bristol B58, 1TH United Kingdom

(Received 27 February 2007; accepted 29 May 2007; published online 13 July 2007)

A composition-temperature phase diagram of the system $(1-x)(K_{0.5}Na_{0.5})NbO_3-xLiNbO_3$ is presented for $0\leqslant x\leqslant 0.1$. Using dielectric and piezoelectric resonance measurements, and Raman spectroscopy, ceramic samples containing 2%–10% $LiNbO_3$ were studied over a temperature range of 7–770 K showing a complex sequence of phase transitions. Analysis of the different Raman, piezoelectric, and dielectric data shows distinct transitions from cubic to tetragonal to orthorhombic to rhombohedral phase for $x=0.02-0.05$. The symmetries of the phases were assigned using analogy to phase diagram of $(K_{0.5}Na_{0.5})NbO_3$ single crystals and ceramics ($x=0$). At $x>0.07$ only one transition between ferroelectric phases occurs where tetragonal phase transforms to another phase, possibly of rhombohedral, orthorhombic, or monoclinic symmetry. In the region between $x=0.05$ and $x=0.08$, the phase transition sequence is more complex. Below 100 K this phase with unidentified symmetry creates a vertical boundary with the rhombohedral phase present near 5% Li. A triple point between the tetragonal, orthorhombic, and the new phase is identified. © *2007 American Institute of Physics*. [DOI: 10.1063/1.2752799]

I. INTRODUCTION

In recent years there is an increasing interest in lead-free piezoelectric ceramics as a possible replacement for $Pb(Zr,Ti)O_3$ (PZT)[1]. Since the excellent electromechanical properties of PZT have been related to a morphotropic phase boundary (MPB) between rhombohedral, tetragonal, and monoclinic phases,[2] strong emphasis has been given on investigating systems containing MPBs. One such system showing enhanced piezoelectric and dielectric properties is $(1-x)(K,Na)NbO_3-xLiNbO_3$ (KNLN). It has been demonstrated that in this system, those properties show a maximum[1,3–5] at around 6%–7% $LiNbO_3$ at room temperature coinciding with a structural transformation from an orthorhombic to a tetragonal phase.[6] This was believed to be the result of an MPB.[1]

In ferroelectric materials the piezoelectric and dielectric coefficients are often enhanced in the vicinity of transitions driven by external fields,[7] temperature,[8] or composition (MPB).[9,10] The enhancement is in each case intimately linked with the flattening of the free energy profile.[11] In PZT, the MPB is nearly vertical in the temperature-composition phase diagram.[9,12] Compositions on each side and in the vicinity of the MPB remain either of tetragonal or rhombohedral (monoclinic) phase on heating while retaining large piezoelectric coefficients at room temperature. Even in those compositions that are very close to the phase boundary at room temperature and which would cross this boundary if temperature is changed, the large piezoelectric response is still dominated by a compositionally driven rather than a temperature driven transition. This can be most clearly seen from phenomenological models based on the Landau theory. These models do not assume temperature driven transitions (a nonvertical boundary is obtained by introducing sixth order terms in the free energy expansion[12]) and show that the origin of properties' enhancement in PZT is compositionally driven flattening of the thermodynamic potential.[10,13,14]

In KNLN and related systems, unlike in PZT, the transition between tetragonal and orthorhombic phases shifts toward lower temperatures when the concentration of $LiNbO_3$ is increased;[15] in the temperature-composition phase diagram the phase boundary between tetragonal and orthorhombic phases is thus not vertical. Such a temperature dependent MPB has also been reported in relaxor-ferroelectric solid solutions, such as $Pb(Mg_{1/3}Nb_{2/3})O_3-PbTiO_3$,[16] $Pb(Zn_{1/3}Nb_{2/3})O_3-PbTiO_3$,[16] and $Pb(Ni_{1/3}Nb_{2/3})-Pb(Zr,Ti)O_3$.[17] In KNLN, maxima in the dielectric and piezoelectric responses are observed around room temperature coinciding with the thermally induced orthorhombic-tetragonal phase transition temperature.[15] Thus, a question can be posed whether the enhanced room temperature properties in KNLN and related solid solutions are dominated by instabilities associated with the proximity of the phase transition temperature or, as most often claimed, are a consequence of a compositionally driven phase transition (an MPB). This issue is relevant for applications because a maximum in properties dominated by a temperature driven phase transition would have, as a consequence, a severe tempera-

[a]Electronic mail: naama.klein@epfl.ch
[b]Permanent address: MacDiarmid Institute of Advanced Materials and Nanotechnology, Victoria University of Wellington, Wellington, New Zealand.

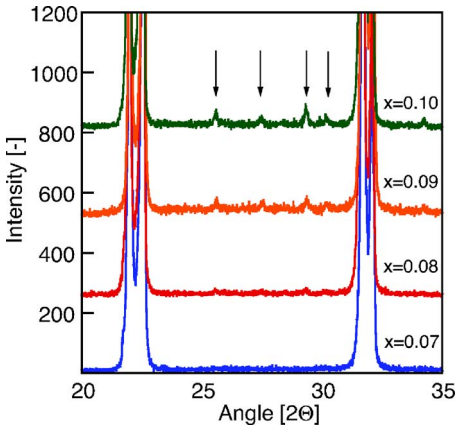

FIG. 1. (Color online). X-ray diffraction spectra of KNLN with $x=0.07-0.10$, showing a gradual appearance of traces of a secondary phase. The secondary phase peaks are marked by arrows. Peaks of the main phase reach a maximum of 3500 in intensity.

ture sensitivity, as indeed has been reported in the literature.[18] In addition, a temperature variation could lead to partial depoling due to a change of the domain configuration when the sample crosses the phase transition temperature and changes its crystal structure. A thorough delineation of the phase transitions in KNLN and related systems is essential to get a deeper insight into the nature of this problem. In this study we propose a tentative temperature-composition phase diagram of $(1-x)(K_{0.5}Na_{0.5})NbO_3-xLiNbO_3$ solid solution for $0 \leqslant x \leqslant 0.1$, based on dielectric permittivity, piezoelectric resonance, and Raman spectroscopy measurements of ceramic samples ($x \geqslant 0.02$). The transition temperatures for undoped $(K_{0.5}Na_{0.5})NbO_3$ (KNN) are taken from the literature.[9]

II. SAMPLE PREPARATION

Ceramics of $K_{1/2-x/2}Na_{1/2-x/2}Li_xNbO_3$ (abbreviated $100x\%$ Li, with $x=0.02$, 0.03, 0.04, 0.05, 0.06, 0.07, 0.08, 0.09, 0.1) were prepared by solid state synthesis from K_2CO_3 99.997%, Na_2CO_3 99.997%, Li_2CO_3 99.999%, and Nb_2O_5 99.9985% starting powders which were dried at 473 K. The raw powders were weighed according to the desired composition and mixed with the aid of ZrO_2 balls for 24 h in isopropanol. After separating the balls and drying, the powders were calcined twice at 1073 K for 4 h, grinding with a mortar and pestle before each calcination. The final powders were then pressed to 7 and 9 mm diameter pellets and sintered in air at temperatures ranging between 1328 and 1368 K with a dwell time of 10 min. The grain size of sintered ceramics was homogenous and below 15 μm. In agreement with the results of Guo *et al.*,[4] we have seen by x-ray diffraction a gradual appearance of traces of a secondary phase in compositions with $x>0.07$. However, even for $x=0.1$ (see Fig. 1), this phase is present only in a small amount which does not affect our analysis of phase transition sequences. The compositions with $x=0.04-0.08$ were analyzed using Inductively Coupled Plasma Mass Spectrometry. The difference between measured and nominal concentrations is less than 1 at. % for Li. The samples are slightly deficient in K and Na, up to 2 at. %, but with K/Na ratio equal to the nominal. The sintered samples, with densities between 91%–96% of the theoretical density, were polished to the final size keeping the aspect ratio of the samples (thickness/diameter) smaller than 0.1, suitable for dielectric and piezoelectric measurements. Gold-chromium electrodes were sputtered on both parallel surfaces for these electrical measurements.

III. EXPERIMENTAL PROCEDURE

The relative permittivities of the unpoled samples at constant stress ε_{33} and loss tangent δ were determined from capacitance measurements using a high precision bridge HP4284A. Measurements were made at a frequency of 100 kHz, upon heating the samples from 303 to 773 K at 2 K/min. Since dielectric anomalies associated with ferroelectric-ferroelectric phase transitions appearing at lower temperatures are broad, the temperatures of those transitions were sometimes difficult to determine. The accuracy may be improved by measuring permittivity and loss of poled samples or by taking temperature derivatives of permittivity and loss data.[17] Therefore the samples were poled at 323 K and under 50 kV/cm for different times ranging from 5 to 30 min optimized for the different compositions. After aging for at least 24 h, the relative permittivity was measured again upon heating from 33 to 473 K using the same parameters. The accuracy in the determination of the phase transition temperatures is estimated to be about 4 K.

Poled samples were also used to determine phase transition temperatures by observing anomalies in the elastic properties via the piezoelectric resonance technique.[9] Elastic anomalies are sometimes more distinct and less ambiguous than dielectric anomalies, which can be caused by charge relaxation processes as well as by structural phase transitions. Furthermore elastic properties in ferroelectrics may be sensitive to structural modifications that do not leave a clear signature in the dielectric behavior. Such is the case for the transition between the low and high temperature rhombohedral phases in Zr rich PZT (Ref. 19) and for ferroelectric-paraelectric phase transition in $Gd_2(MoO_4)_3$.[20] Resonant (minimum of impedance) and antiresonant (maximum of impedance) frequencies of the fundamental radial vibrations were determined using an impedance analyzer upon heating in the temperature range from about 100 to 420 K. The samples were stabilized at each temperature for at least 5 min.

For the radial mode, the resonant frequency under a short circuit condition is related to elastic properties[21] by $f_r \propto (1/r)\sqrt{1/\rho s_{11}^E(1-\sigma)^2}$, where r is the radius of the sample, ρ its density, σ the Poisson ratio, and s_{11}^E is the elastic compliance. For the present purposes it was not necessary to calculate explicitly the elastic coefficients since the temperature dependence of the resonant frequencies is sufficient to determine the phase transition temperatures. The accuracy in the determination of the phase transition temperatures is estimated to be about 10 K, equal to temperature intervals between measurements.

Unpolarized Raman spectroscopy was conducted using a Renishaw InVia Raman microscope with the polished samples enclosed in a Linkam THMSG 600 variable tem-

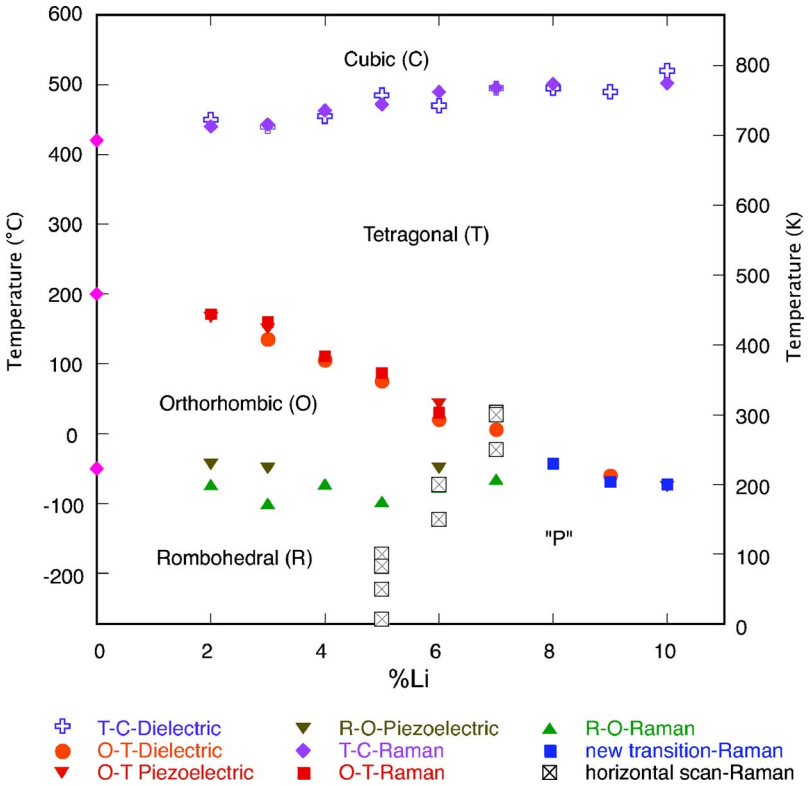

FIG. 2. (Color online) Temperature-composition phase diagram of $(1-x)(K_{50}Na_{50})NbO_3-xLiNbO_3$ solid solution for $0 \leqslant x \leqslant 0.1$, based on dielectric permittivity, piezoelectric resonance, and Raman spectroscopy measurements of ceramic samples ($x \geqslant 0.02$), revealing the presence an unknown phase (P) which maintains a vertical boundary with the rhombohedral phase. A triple point where T, P, and O phases meet is seen at around $x=0.07$.

perature stage for data above 80 K, and in a liquid He flow Oxford microcryostat for lower temperatures. The 488 nm line of an Ar laser was used as excitation source for the measurements. The illuminated spot at the sample was of about 0.5–0.7 μm diameter. Laser power was kept to less than 1 mW, which limited laser heating of the samples to less than the temperature resolution used (5 K). Spectra were taken on heating the samples from 7 to 820 K.

In many cases the spectra across a phase boundary were clearly and qualitatively different at a level that could be noted as the data were collected. However, across some transitions the changes were more subtle, as will be seen below, and for those it was necessary to characterize the changes with more sensitivity. For that purpose the spectra were first normalized to their integrated intensities to eliminate effects associated with the inevitable ~10% variation introduced by refocusing, and those normalized spectra were fitted with an appropriate number of Lorentzian lines. We then sought signatures of phase changes in the temperature and composition dependence of the line frequencies, widths, and strengths.

We emphasize that all techniques were used as empirical tools to identify phase changes. Thus, for example, in the analysis of Raman spectra no attempts have yet been carried out to identify the normal modes responsible for the features ascribed to different phases. Another important remark is that all temperatures quoted in this work were taken from data obtained on increasing temperatures. This was done for reasons of consistency, because tetragonal-cubic and orthorhombic-tetragonal phase transitions exhibited a considerable thermal hysteresis.

IV. RESULTS AND DISCUSSION

To facilitate the data analysis presented in Secs. IV A–IV F, the derived phase diagram is first shown in Fig. 2. In analogy with the phase diagram of KNN ($x=0$) (Ref. 9), we identify different phases to be, below 5%Li, cubic (C), tetragonal (T), orthorhombic (O), and rhombohedral (R). It should be mentioned that a recent study has suggested a monoclinic symmetry for the room temperature phase of KNN.[22] Raman spectra (Sec. IV E) show that the low temperature phase in samples with $x>5\%$ is different from the R phase. This phase is referred to as "P" phase.

A. Phase transitions determined from permittivity data

The temperature dependence of the relative permittivity shows two clear peaks that were associated with phase transitions. A third peak is observed at low temperatures in some compositions with $x<0.07$. This peak is less pronounced than the two peaks appearing at higher temperatures, but can be seen in the temperature derivative of the permittivity. That this third dielectric peak is related to a phase transition is confirmed by the Raman and/or piezoelectric data discussed later. Figure 3 shows dielectric peaks for samples with $x=0.03$ and 0.09 in the temperature range from 100 to 800 K. The peak present at the higher temperature corresponds to the T-C phase transition. Its temperature increases gradually from about 673 at 2%Li to 773 K at 10%Li. The temperature of the second peak, seen at 453 K for 3%Li, shifts to lower temperatures with increasing x; it becomes wider and less well defined as Li concentration increases, as illustrated in Fig. 3 for composition with $x=0.09$.

B. Piezoelectric resonance measurements

Resonant and antiresonant frequencies were measured for samples with 2%, 3%, 5%, 6%, and 10%Li. A typical temperature dependence is plotted as a function of tempera-

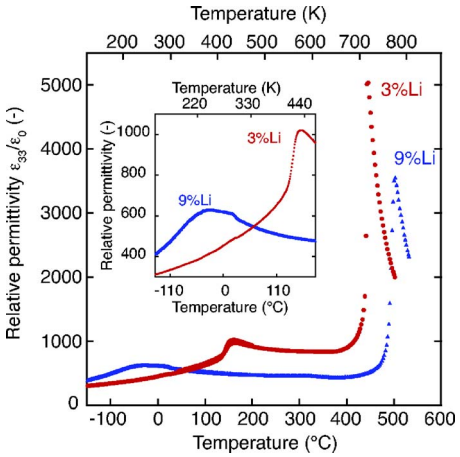

FIG. 3. (Color online) Temperature dependence of the relative permittivity of KNLN with $x=0.03$ and $x=0.09$ measured at 100 kHz. The inset shows enlarged region where *O-T* phase transition occurs.

ture in Fig. 4, for samples with $x=0.02$ and $x=0.06$. These plots enable identification of the phase transitions via two main characteristics. The transitions in the 2%Li sample [Fig. 4(a)] are indicated by a nearly discontinuous jump of characteristic frequencies of about 0.5 MHz at ~420 K and a more gradual increase of about 0.3 MHz at ~210 K. In the 6%Li sample [Fig. 4(b)], phase transitions are denoted by a large change of the slopes of the resonant frequency versus temperature curves, at ~290 and ~210 K. The low temperature transition in both cases occurs over a temperature range of about 30 K. In addition to phase transitions, a softening of the structure is indicated in Fig. 4(b) by a slow decrease in the resonant frequencies above 350 K.

C. Raman spectroscopy: Qualitative inspection

Very distinct spectral changes across the *T-C* phase transition boundary are apparent, as discussed for the 7%Li sample and shown in Fig. 5(a). Just below the transition the *T* phase has strong broad lines at 250 and 600 cm^{-1} and a weaker line at 850 cm^{-1}. The two strong lines broaden and weaken above the Curie temperature T_C at 720 K, and the weak line disappears completely. These changes were found to be universal in the KNLN system, including in Li-free single crystals[23] and $KNbO_3$ ceramics,[24] making this transition especially easy to trace by Raman spectroscopy. The

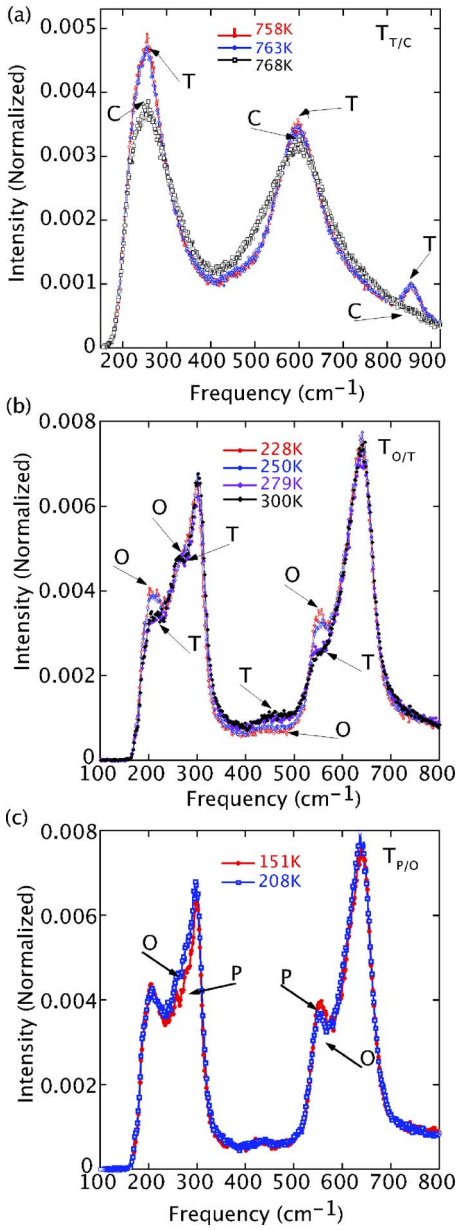

FIG. 5. (Color online) Raman spectra of KNLN sample with $x=0.07$ going through a sequence of phase transitions (a) *T-C*, (b) *O-T*, and (c) *P-O*.

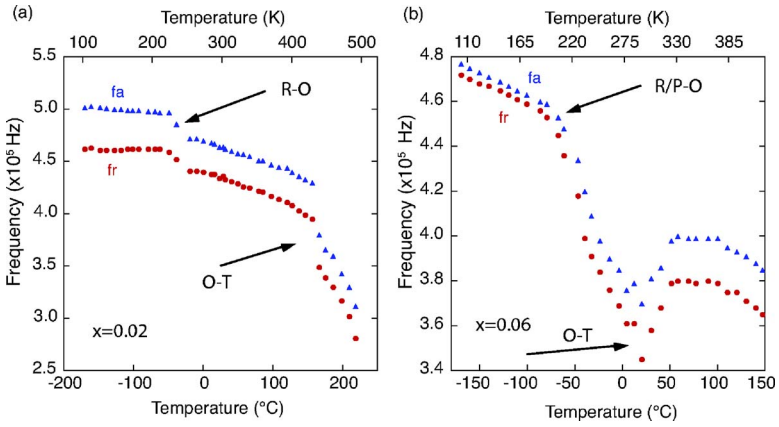

FIG. 4. (Color online) Temperature dependence of the radial mode resonant and antiresonant frequencies for KNLN samples with (a) $x=0.02$ and (b) $x=0.06$. The arrows indicate positions of *R/P-O* and *O-T* phase transitions.

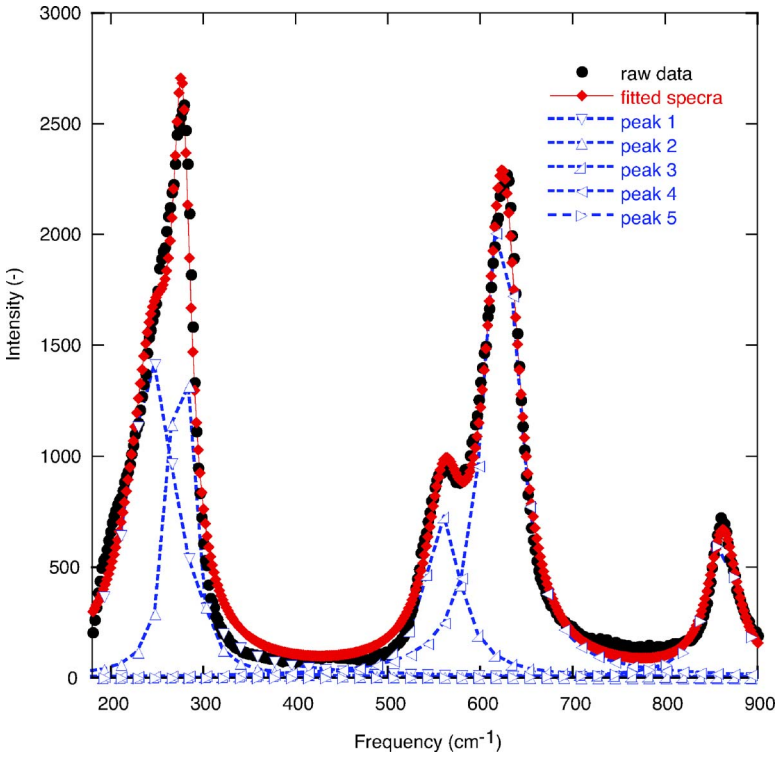

FIG. 6. (Color online) Fitted Raman spectra of KNLN sample with $x=0.03$, where the circles are the raw experimental data, the triangles are Lorentzian fits of individual peaks, and the diamond shapes are the total spectrum calculated from fitted data. The lines are guides for the eye.

cubic perovskite phase, with all ions at centers of inversion, supports no Raman active modes at all. Subsequently, the presence of any Raman signal above T_C establishes that the phase has significant local departures from a cubic perovskite structure.[25]

The next transition below the Curie temperature of the 7%Li sample is depicted in Fig. 5(b). It should be noted that the Raman signature of the *T* phase differs between Figs. 5(a) and 5(b), as should be expected in view of the factor of 2 difference in the temperatures at which they were taken. At 300 K the *T*-phase Raman spectrum shows lines that have narrowed substantially from 750 K, now showing multiple phonon contributions to the two main features found at 250 and 600 cm^{-1} in the 770 K spectrum. In addition to the narrowing, all of the phonons harden, i.e., increase in frequencies, as the temperature is lowered, as is expected for thermal contraction. We have followed the evolution of the Raman spectra with temperature across the entire *T* phase, establishing the absence of any discontinuous changes that would signal a further phase transition.

In the *O* phase there are distinct shoulders in the Raman spectra on the low-frequency sides of the main Raman modes, shoulders that are present also in the *T* phase although rather weaker. Furthermore, the *O* phase sees a loss in Raman intensity in the 400–500 cm^{-1} region. As can be seen in Figs. 5(b) and 5(c), the *P*-*O* transition has similar characteristics to the *O*-*T* transition. The same lines exist, but they show a discontinuous change in relative intensity across the *P*-*O* phase transition. Thus extracting these transition temperatures requires a more careful fitting of the Raman spectra.

Samples with $x<0.05$ show the same features as 7%Li sample except that the low temperature phase is *R* and not *P*. The difference between *R* and *P* phases will be evident from the analysis in Sec. IV E. In compositions with *x* above 0.07–0.08, only one phase transition between ferroelectric phases (*P*-*T*) is observed.

D. Fittings of Raman spectroscopy data

The Raman spectra were fitted using a sum of Lorenzian lines. This is illustrated in Fig. 6 for the example of the 3%Li sample. The fitted line corresponds well to the raw data with $R^2>99\%$. Information on width, intensity, and frequency position of the peaks was extracted from the fitted curves and is shown as a function of temperature in Fig. 7. Data for samples with a $LiNbO_3$ concentration in the range of 2%–6% indicate only one phase transition below room temperature, characterized by a change in the slope of the temperature dependence of the phonon frequencies [Figs. 7(a) and 7(b)]. The phase transition temperature was determined as the temperature at which the two lines from the different slopes intersect. After extrapolation to Li-free KNN ($x=0$), this phase transition is tentatively identified as the *R*-*O* phase transition. The gradual change of the phonon properties and the absence of perceptible thermal hysteresis between *R* and *O* phases would suggest a second order phase transition. The second order signature is surprising considering the discontinuous character of this transition in KN and KNN crystals.[23,26]

Assuming the same phases as in KN and KNN (with cubic $Pm\bar{3}m$, tetragonal 4*mm*, orthorhombic *Amm*2, and rhombohedral *R*3*m* symmetries), the second order character of this phase transition would not agree with group theory predictions.[27,28] Even considering the uncertainty in the symmetry of the *O* phase in KNN and assuming that it could be monoclinic *Pm* nor *P*2 as proposed in Ref. [22], a transition to the rhombohedral phase should not be of second order.[27,28]

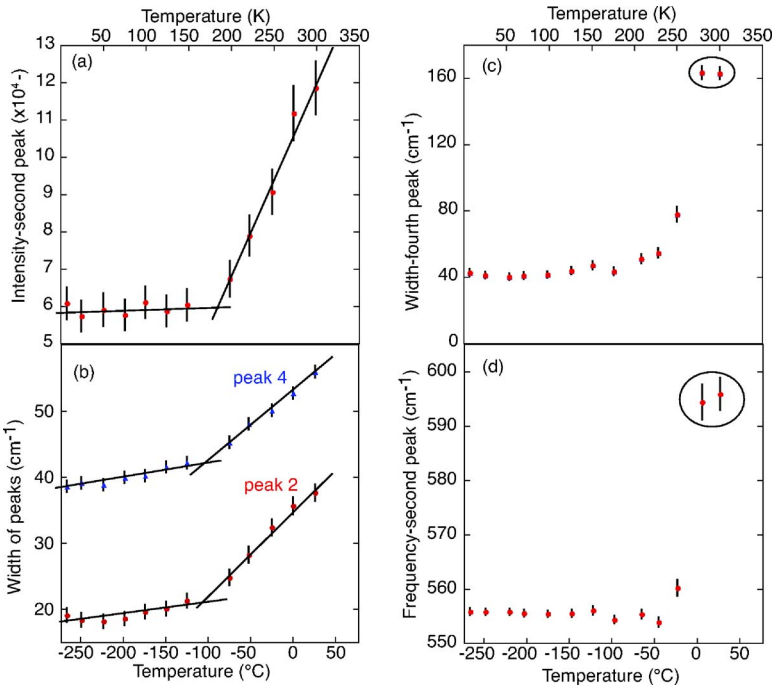

FIG. 7. (Color online) Width, intensity, and position of fitted Raman peaks as a function of temperature for KNLN sample with $x=0.03$ [(a) and (b)] and $x=0.07$ [(c) and (d)]. The vertical lines denote error bars.

Thus, it is more likely that this transition is of the first order, and that a discontinuity is not seen because of limitations in the measurement resolution. An alterative explanation could be that the space group of Li-modified compositions may not be the same as for KN and KNN; this can happen if, for example, addition of Li induces tilt of oxygen octahedra.[27] However, a first order assignment for this phase transition is supported by the fact that in samples with a higher Li content the transition has first order features, as illustrated for samples with $x=0.07$ in Figs. 7(c) and 7(d) near 250 K. Here an abrupt change in the fitted parameters is clearly apparent, consistent with the prediction of a first order phase transition. As shown below, this phase is not the same as the *R* phase just described.

E. Isothermal or composition-dependent lines

Normalized Raman spectra from all concentrations at constant temperature were analyzed. Examples of spectra are shown in Fig. 8 for 7, 300, 470, and 670 K. Figure 8(a) is representative of what is seen below 100 K. It reveals an abrupt change of pattern between 5% and 6% $LiNbO_3$, with a line at 280 cm^{-1}, identifying the *R* phase at lower Li concentrations, developing satellites in the region between 200 and 280 cm^{-1}, and indicating the appearance of a new phase denoted as *P*. This phase transition between the *R* and *P* phases is vertical (temperature independent). Above 100 K the temperature of this phase transition gradually shifts until at 273 K it passes between 6% and 7%Li [Fig. 8(b)]. Above room temperature there is no sign for a phase transition of this type [Figs. 8(c) and 8(d)].

F. The phase diagram

The phase diagram, Fig. 2, shows excellent agreement between phase transition temperatures determined by different methods. We call attention to the following.

(i) The crystal phases are identified in analogy to the phases known for $K_{0.5}Na_{0.5}NbO_3$ ($x=0$). This analogy, however, is possible only for compositions below about $x=0.05$. At higher concentrations of Li, another phase appears at low temperatures, marked by *P* in the diagram. As mentioned before, the orthorhombic symmetry at room temperature in $K_{0.5}Na_{0.5}NbO_3$ has been questioned; it has been proposed, partly based on Raman spectroscopy data, that the actual phase is monoclinic in powders with grain size >200 nm.[22]

(ii) Our data suggest that a vertical MPB appears at approximately $x=0.05$, at temperatures below ~ 100 K. At higher temperatures and up to 273 K this boundary bends toward $x=0.07$. The boundary separates the *R* phase of $K_{0.5}Na_{0.5}NbO_3$ and the *P* phase identified in this work.

If the two phases on each side of the MPB exhibit such symmetries that their polarization orientation is different (e.g., rhombohedral and monoclinic or rhombohedral and orthorhombic phases), then the nature of this MPB would be similar to that in relaxor-ferroelectric crystals or in PZT,[29] where the huge enhancement of the piezoelectric properties along nonpolar directions is related to the polarization rotation mechanism.[30] The vertical MPB in KNLN appears at temperatures that are too low to be of wide-range practical interest and where the magnitude of the materials coefficients would be in any case low. However, its presence is important from the fundamental point of view: it would signal the possibility that this lead-free system supports such MPBs, which may be brought to a more useful temperature range by modifying crystal composition.

Another possibility is that the *R* and *P* phases are variations of the same symmetry. Apart from the suggestion in Ref. 22 that the room temperature phase of

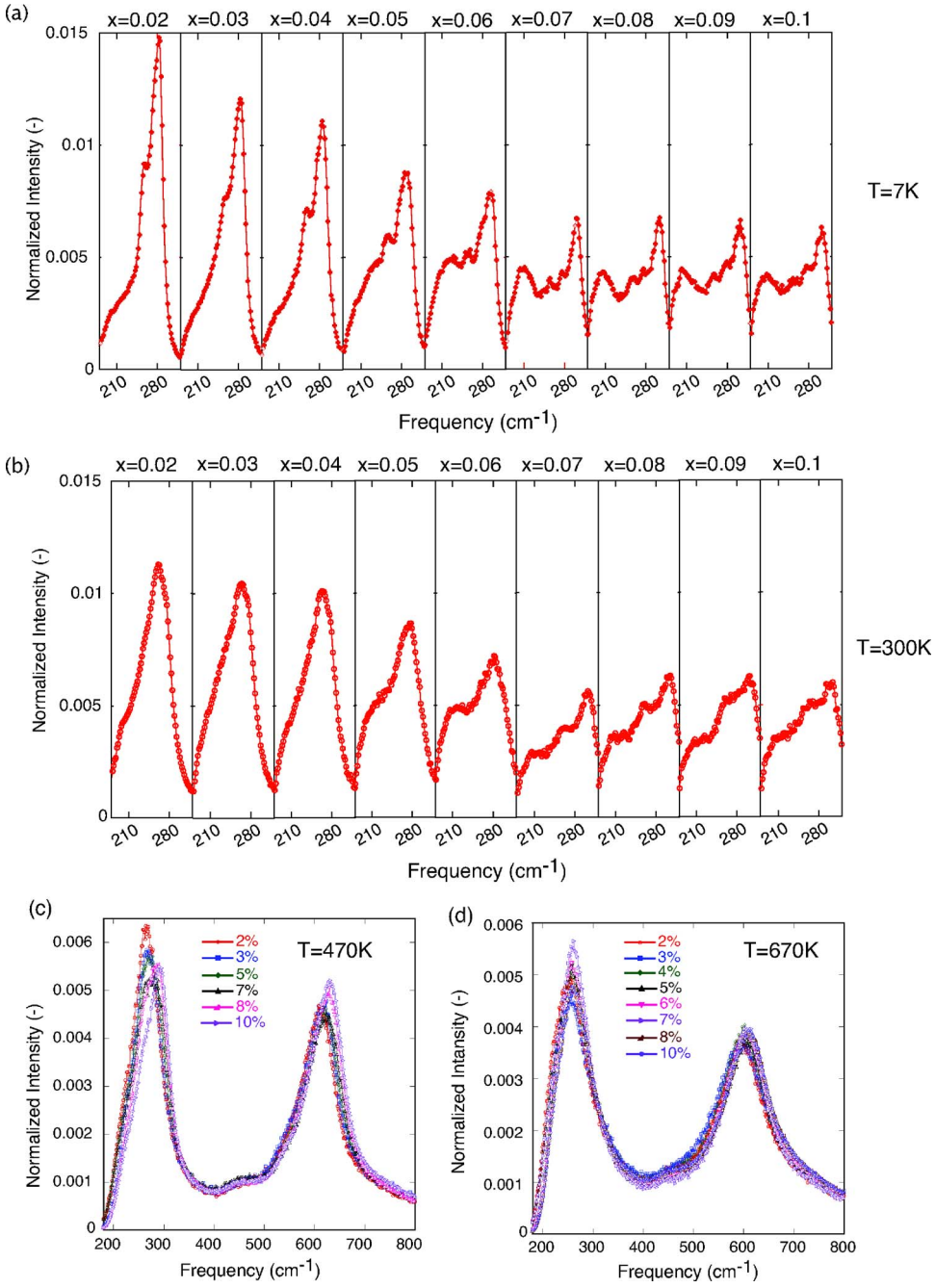

FIG. 8. (Color online) Normalized Raman spectra of different compositions showing a phase transition around (a) $x=0.05$ at 7 K, (b) $x=0.07$ at 300 K, and no transitions at (c) 470 K and (d) 670 K.

$K_{0.5}Na_{0.5}NbO_3$ is monoclinic, a vertical morphotropic phase boundary between two orthorhombic phases has been reported at approximately $y=0.5$ (Ref. 9) in the $K_{1-y}Na_yNbO_3$ phase diagram. The vertical boundary at $x=0.05$ in Fig. 2 could correspond to such a phase boundary, possibly separating two rhombohedral phases.

(iii) The phase diagram exhibits a region at $x \approx 0.07-0.08$ and $\sim 223-273$ K, where three phases (P, O, and T) meet. Such a region, in which two or more phases have a nearly degenerate energy is associated with a flat free energy profile, possibly leading to enhanced piezoelectric and dielectric properties.[10,11,31] Their enhancement in this part of the phase diagram needs to be confirmed experimentally. Like the vertical MPB discussed in (ii), such a region could hopefully be brought to a more useful temperature range by crystal chemistry engineering.

V. CONCLUSIONS

We have proposed a phase diagram of the system $(1-x)(K_{0.5}Na_{0.5})NbO_3-xLiNbO_3$ based on dielectric and piezoelectric measurements, and Raman spectroscopy. Our results suggest the presence of a vertical MPB at low temperatures at approximately $x=0.05$. This boundary separates a rhombohedral phase, possibly the same as the one observed in $(K_{0.5}Na_{0.5})NbO_3$, and another phase whose crystal structure could not be revealed in the present measurements, needing further investigation. The results also identify a triple point where tetragonal, the unknown phase, and the

orthorhombic phase meet. Both the vertical MPB and the triple point are regions where enhanced piezoelectric and dielectric properties can be expected. Their present low temperature range could likely be increased by chemical engineering into practically used temperature ranges.

Note added in proof. After the manuscript was submitted it was found using x-ray diffraction that the symmetry of the "P" phase is monoclinic. Results of X-ray diffraction experiments, made in collaboration with B. Dkhil and P. Gemeiner from Ecole Central Paris, will be reported elsewhere.

ACKNOWLEDGMENTS

The authors would like to thank Dr. J. W. Pomeroy and Dr. A. Sarua (University of Bristol) for contributions to the Raman measurements. This work was carried out in the framework of the European CRAFT project IMMEDIATE. The European COST 539 Program is acknowledged for travel support. Inductively Coupled Plasma Mass Spectrometry analysis was carried out at the Institute of Mineralogy and Geochemistry, University of Lausanne, Switzerland.

[1]Y. Saito, H. Takao, T. Tani, T. Nonoyama, K. Takatori, T. Homma, T. Nagaya, and M. Nakamura, Nature (London) **432**, 84 (2004).
[2]B. Noheda, Curr. Opin. Solid State Mater. Sci. **6**, 27 (2002).
[3]S.-Y. Chu, W. Water, Y.-D. Juang, and J.-T. Liaw, Ferroelectrics **287**, 23 (2003).
[4]Y. Guo, K. I. Kakimoto, and H. Ohsato, Appl. Phys. Lett. **85**, 4121 (2004).
[5]E. Hollenstein, M. Davis, D. Damjanovic, and N. Setter, Appl. Phys. Lett. **87**, 182905 (2005).
[6]K. Kakimoto, K. Akao, Y. Guo, and H. Ohsato, Jpn. J. Appl. Phys., Part 1 **44**, 7064 (2005).
[7]Z. Kutnjak, J. Petzelt, and R. Blinc, Nature (London) **441**, 956 (2006).
[8]D. Viehland, A. Amin, and J. F. Li, Appl. Phys. Lett. **79**, 1006 (2001).
[9]B. Jaffe, W. R. Cook, and J. H. Jaffe, *Piezoelectric Ceramics* (Academic, New York, 1971).
[10]Y. Ishibashi and M. Iwata, Jpn. J. Appl. Phys., Part 1 **38**, 800 (1999).
[11]M. Budimir, D. Damjanovic, and N. Setter, Phys. Rev. B **73**, 174106 (2006).
[12]Y. Ishibashi and M. Iwata, Jpn. J. Appl. Phys., Part 2 **37**, L985 (1998).
[13]D. Damjanovic, J. Am. Ceram. Soc. **88**, 2663 (2005).
[14]M. J. Haun, E. Furman, S. J. Jang, and L. E. Cross, Ferroelectrics **99**, 63 (1989).
[15]M. Matsubara, T. Yamaguchi, K. Kikuta, and S. I. Hirano, Jpn. J. Appl. Phys., Part 1 **44**, 6136 (2005).
[16]B. Noheda, Curr. Opin. Solid State Mater. Sci. **6**, 27 (2002).
[17]G. Robert, M. Demartin, and D. Damjanovic, J. Am. Ceram. Soc. **81**, 749 (1998).
[18]S. Zhang, R. Xia, T. R. Shrout, G. Zang, and J. Wang, J. Appl. Phys. **100**, 104108 (2006).
[19]D. Berlincourt, H. H. A. Krueger, and B. Jaffe, J. Phys. Chem. Solids **25**, 659 (1964).
[20]L. E. Cross, A. Fouskova, and S. E. Cummins, Phys. Rev. Lett. **21**, 812 (1968).
[21]IEEE Standard on Piezoelectricity ANS/IEEE Std. 176-1987, 1988; IEEE Trans. *UFFC*, Vol. 40 (1988).
[22]Y. Shiratori, A. Magrez, and C. Pithan, J. Eur. Ceram. Soc. **25**, 2075 (2005).
[23]H. J. Trodahl, N. Klein, and D. Damjanovic (unpublished).
[24]J. A. Baier-Saip, E. Ramos-Moor, and A. L. Cabrera, Solid State Commun. **135**, 367 (2005).
[25]J. Rouquette, J. Haines, V. Bornand, M. Pintard, P. Papet, R. Astier, J. M. Leger, and F. Gorelli, Phys. Rev. B **65**, 214102 (2002).
[26]G. Shirane, R. Newnham, and R. Pepinsky, Phys. Rev. **96**, 581 (1954).
[27]H. T. Stokes, E. H. Kisi, D. M. Hatch, and C. J. Howardc, Acta Crystallogr., Sect. B: Struct. Sci. **B58**, 934 (2002).
[28]J. S. Forrester, R. O. Piltz, E. H. Kisi, and G. J. McIntyre, J. Phys.: Condens. Matter **13**, L825 (2001).
[29]B. Noheda and D. E. Cox, Phase Transitions **79**, 5 (2006).
[30]S. E. Park and T. R. Shrout, J. Appl. Phys. **82**, 1804 (1997).
[31]Z. Wu and R. E. Cohen, Phys. Rev. Lett. **95**, 037601 (2005).